

Influence of sinter-cooling rate on the mechanical properties of powder metallurgy austenitic, ferritic, and duplex stainless steels sintered in vacuum

F. Martín^{a,*}, C. García^a, Y. Blanco^a, M.L. Rodríguez-Mendez^b

^a Materials Engineering, E.I.I., Universidad de Valladolid, C/Paseo del cauce 59, 47011 Valladolid, Spain

^b Department of Inorganic Chemistry, E.I.I., Universidad de Valladolid, C/Paseo del cauce 59, 47011 Valladolid, Spain

ARTICLE INFO

Article history:

Received 16 May 2015

Accepted 30 June 2015

Available online 9 July 2015

Keywords:

Mechanical characterization

Hardness measurement

Steel

Powder metallurgy

Hardening

ABSTRACT

Austenitic, ferritic and duplex stainless steels obtained through powder metallurgy technology were sintered in vacuum. Powders were compacted at 650 or 750 MPa and sintered in vacuum with two sinter-cooling rates (furnace- and water-cooling). Mechanical properties, using tensile testing and hardness measurements were evaluated. A full microstructural study of the three types of stainless steels was performed. The mechanical behavior was a function of the sinter-cooling rate and the chemical composition. Duplex stainless steel showed the best mechanical behavior. The use of high compaction pressure and water-cooling process promoted the best mechanical results for all compositions.

© 2015 Elsevier B.V. All rights reserved.

1. Introduction

Powder metallurgy (PM) stainless steel (SS) components constitute an important and growing segment of the PM industry. Austenitic grades have been widely used in automotive, marine, food, biomedical industries due to their high corrosion resistance [1]. However, ferritic SS have gained wide acceptance in automotive exhaust systems, containers and other functional applications owing to good fabrications at low cost, and their resistance to corrosion and oxidation [2–4]. Conventional (non-PM) duplex stainless steels have a combination of mechanical strength, toughness and corrosion resistance that make them attractive for numerous applications [5]. For duplex PM SS is also possible to achieve a high corrosion resistance [6].

PM stainless steels, as compared to their equivalent non porous materials, show restrictions in their applications due to the relatively poor mechanical and corrosion properties [7]. Therefore, there is always a thrust to improve such properties [8–10].

For PM austenitic SS, there were attempts to increase densification by supersolidus liquid phase for SS sintered in hydrogen atmosphere [11] or by increasing nitrogen sintering temperature to increase tensile and fatigue strengths [11] or, finally, by additions of elements such as silicon to promote the densification rate [12].

It has been reported some results on the nanoindentation

* Corresponding author. Fax: +34 983184514.

E-mail address: fmp@eii.uva.es (F. Martín).

hardness of some PM duplex SS sintered in a vacuum and slow sinter-cooling [13]. It has been explained by the solid solution hardening in ferrite, because of the internal strain hardening between ferrite and austenite and because of the new inter-diffusion area at particles boundary [13]. Furthermore, the copper [14,15] and boron [16] additions, which activate sintering and enhance densification, closing the residual porosity and increasing ductility, improves the mechanical behavior.

PM austenitic and ferritic SS sintered in vacuum show a simple microstructure of austenite and ferrite respectively [17,18]. However, PM duplex SS shows complex microstructures that have been often analyzed by using the Schaffler's diagram. Non-conventional microstructural features such as the mixed constituent can be due to the combined content of alpha-genic and gamma-genic elements that at sintering temperatures show high diffusivity [16,19,20]. Another phenomenon found in PM duplex SS is related to the presence of sigma phase, carbides and other intermetallic compounds [21].

It is clear that the microstructure is influenced by the sinter-cooling rate. Austenitic and ferritic SS sintered in vacuum and after slow cooling during sintering (average cooling rate of 5 °C/min) showed the presence of brittle phases resulting in a decrease of the corrosion resistance [6]. Therefore, it is advisable to avoid these undesirable metallurgical transformations. Powder injection molded 316L, sintered in a vacuum with a cooling rate of 10 °C/min, showed higher mechanical properties and corrosion resistance than those cooled at 5 °C/min [22].

For PM duplex SS sintered in vacuum the effects of sinter-

cooling rate on mechanical properties and corrosion resistance have been partially investigated. The “sinter-hardening” proposed by Dobrzanski et al. [23,24] and cooling with N₂, proven its advantage for corrosion properties but the effect on mechanical behavior was not investigated.

Previous works of the authors [25,26] report that PM SS sintered in nitrogen have proven that nitrogen abortion causes the formation of chromium nitride precipitates, which reduces ductility and promotes chromium depleted areas. The dissolution of these secondary phases by a post-sintered solution annealing is possible. Water quenching from sintering temperature is another possible way to avoid these brittle precipitates [27,28]. Mechanical properties of PM SS sintered in nitrogen has been previously published by the authors [28].

The main issue of the present study is to investigate the microstructure and mechanical properties of stainless steels sintered in vacuum and sinter-cooled at slow and high rates. Three typical PM SS has been chosen, specifically a ferritic 430L, an austenitic 316L and a duplex 50% ferrite powder and 50% austenite powder.

2. Experimental

Two prealloyed and water atomized powders were used as raw materials: AISI 430L (0.018 wt% C, 1.16 wt% Si, 0.18 wt% Mn, 16.9 wt% Cr, 0.10 wt% Ni, Fe bal.) and AISI 316L (0.021 wt% C, 0.87 wt% Si, 0.20 wt% Mn, 16.1 wt% Cr, 13.55 wt% Ni, 2.24 wt% Mo, 0.02 wt% Cu, 0.1%V, Fe bal.). The powder characteristics of AISI 430L were: apparent density 3.0 g/cm³, flow rate 26 s/50 g and nominal particle size < 50 μm. The powder characteristics of AISI 316L were: apparent density 3.1 g/cm³, flow rate 25 s/50 g and nominal particle size < 150 μm. The duplex SS was obtained by premixes of 316L and 430L prepared in a turbular mixer. The content of AISI 316L/430L was set to 50/50 wt%. This material was designated as 50DSS and the two simple materials (430L and 316L) were labeled as base materials.

Dog-bone tensile test specimens [29] were uniaxially compacted using a floating die at selected compaction pressures for selected compaction times. Zinc stearate was used as die lubricant. Compactions at 650 and 750 MPa for 300 s were chosen. Sintering in vacuum (11 Pa) at 1250 °C for 1 h was set. It was found by chemical analysis that there were no chromium losses. After sintering, two different sinter-cooling processes were applied. Some samples were cooled at a slow rate of 5 °C/min in the sintering furnace (referred to from now on as “furnace-cooling” process). Some others were submitted to fast cooling by direct immersion in water (designated from now on as “water-cooling” process). The specimens were referred to as “furnace-cooled” and “water-cooled” samples, respectively.

Image analysis was used to study the porosity of polished samples. Seven fields were taken per sample. Images were digitized and calibrated. The pores were identified as the black pixels and they were computed to calculate the area of each pore.

Samples were polished and etched before observation by optical metallography. The electrochemical etching with oxalic acid (ASTM A262, Practice A [30]) helped to define the location of the chromium precipitates. X-ray diffraction (XRD) was used to identify some of the phases. Finally, the samples were etched with Vilella’s reagent for their analysis by scanning electron microscopy with energy dispersive analysis of X-rays (SEM/EDS).

Tensile tests were performed following the ISO 6892-1 standard [31]. Tensile strength and ductility were evaluated. The apparent hardness (i.e. the value obtained when indentation is the result of plastic deformation of the material and the pores) was evaluated by the Vickers method, using a load of 30 kp (294 N) during 30 s. An average value of five indentations was given as the hardness value.

Table 1
Porosity values for 316L, 430L and 50DSS.

Sample	Compaction pressure (MPa)	Furnace-cooling Porosity (%)	Water-cooling Porosity (%)
316L	750	13.95	14.04
	650	14.96	14.36
430L	750	11.33	10.24
	650	12.10	11.50
50DSS	750	14.2	13.72
	650	15.20	14.83

3. Results

3.1. Porosity and microstructural characterization

The porosity results are collected in Table 1. As expected the higher the compaction pressure the lower the porosity. No significant change in porosity was found from furnace- and water-cooled samples. It can be pointed out that the water-cooled samples show similar or lower porosity than the furnace-cooled specimens.

The microstructure, as expected, is a function of the chemical composition of the samples and the sinter-cooling rate. First, the microstructures of the furnace-cooled samples are discussed and second, the effect of water-cooling is commented. The microstructures are respectively collected in Figs. 1 and 2 for the compaction pressure of 650 MPa. A higher pressure (750 MPa) did not affect to the microstructures; the only difference was a lower degree of porosity (Table 1).

A typical austenitic microstructure with mainly transgranular (TG) precipitates was observed for furnace-cooled 316L (Fig. 1a). For the furnace-cooled 430L (Fig. 1b) a typical ferrite phase with slight intergranular (IG) and TG precipitations were observed. The furnace-cooled 50DSS revealed a more complex microstructure (Fig. 1c), which differed from the austeno-ferritic biphasic structure observed in conventional duplex SS. Austenite and ferrite grains were identified but also a mixed constituent [25], which is in this case a mixture of ferrite and austenite was observed. This mixed constituent was hard to distinguish by conventional optical microscopy and will be latter discussed. In Fig. 1c it can be seen austenite grains with some TG precipitation, ferrite islands and dark areas corresponding to the mixed constituent.

The microstructure of water-cooled 316L was entirely austenitic with a slightly lower grain size than the furnace-cooled 316L (Fig. 2a). There was also a lower amount of precipitation. For water-cooled 430L a higher quantity of precipitates than for 316L was observed (Fig. 2b). Comparing austenitic and ferritic samples, the effect of water-cooling is different, while for 316L the tendency is to obtain a clean microstructure of austenite grains, the contrary is observed for 430L.

For water-cooled 50DSS, the same three constituents as for furnace-cooled was observed but the ratio changed (Fig. 2c). The constituents were: the mixed constituent [25], but in this case is rich in martensite, the austenite grains and some ferrite islands that were in lower amount than for the furnace-cooled. The mixed constituent showed some isolated TG precipitates inside.

Optical microscopy observation is not enough for the full identification of the microstructures, therefore additional techniques such as XRD and SEM/EDS were used. The XRD patterns of all the samples are shown in Fig. 3. The peaks of the austenite phase for 316L were predominant for the two sinter-cooling rate. However, peaks identified as ferrite/martensite phase were also observed and were more significant for the furnace-cooled sample. It is relevant to remind that ferrite and martensite phases have the same peaks in the diffractograms, therefore there is no way to

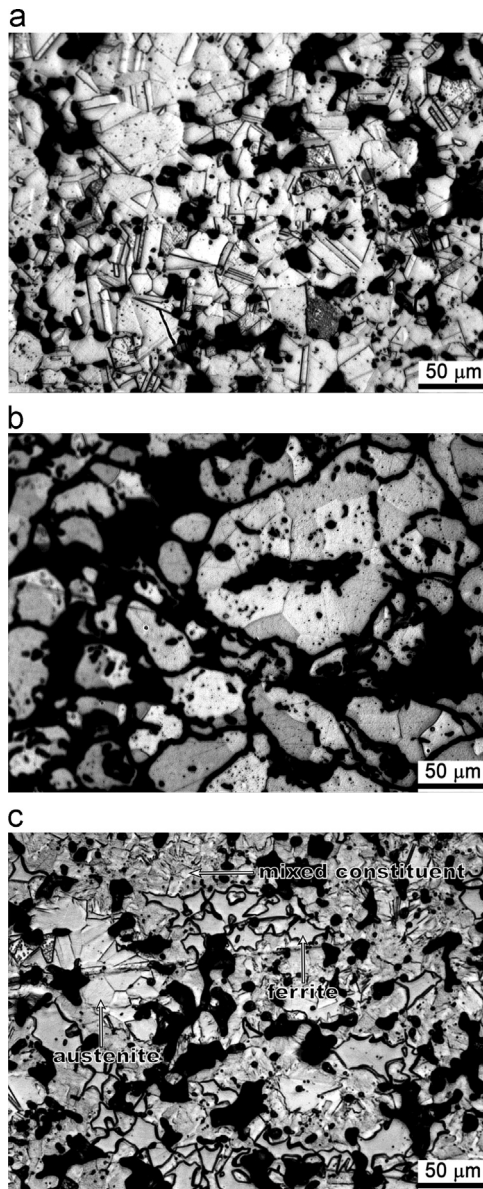


Fig. 1. Optical micrographs of furnace-cooled samples electrochemically etched with oxalic acid and compacted at 650 MPa. (a) 316L, (b) 430L and (c) 50DSS.

discriminate among the two. In addition, traces of carbides (type Cr_7C_3 and Cr_{23}C_6) and oxides, only for furnace-cooled samples, were identified though the peaks are very small to be seen in Fig. 3. The XRD of 430L only showed ferrite peaks and, as for 316L, traces of carbides and oxides were identified for furnace-cooled samples.

For 50DSS samples, the amount of austenite phase was lower than the expected in accordance with the amount of initial austenitic powder. To interpret these results, it must be considered that the ferrite/martensite peaks are present in the ferrite islands and in the mixed constituent. Water-cooled 50DSS exhibited ferrite/martensite peaks with lower intensity, indicating a lower amount of ferrite/martensite, which matches with the lower amount of ferrite islands. XRD of bulk materials has not enough resolution to give information about the type of precipitates. An approach to solving this problem is performing a so-called bulk extraction prior XRD analysis. The metal matrix is electrolytically dissolved with 10% HCl in methanol solution at 5–6 V and the filtered residues (formed by the undissolved precipitates) are XRD analysed (Fig. 3). The amount of precipitates was slightly lower for

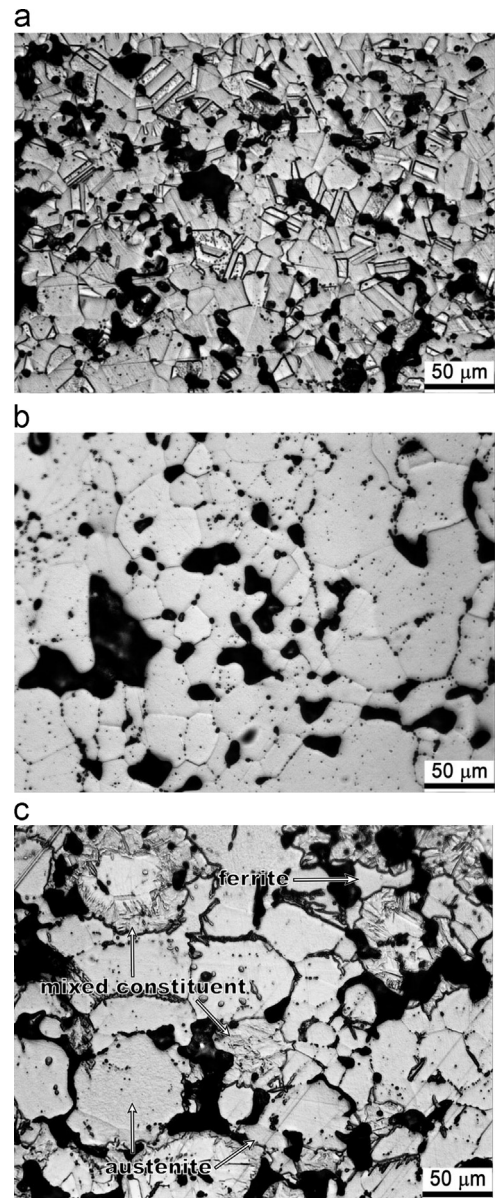


Fig. 2. Optical micrographs of water-cooled samples electrochemically etched with oxalic acid and compacted at 650 MPa. (a) 316L, (b) 430L and (c) 50DSS.

the water-cooled samples but anyhow, for both sinter-cooling rates, the amount of precipitates was relatively small.

SEM/EDS was used to identify some constituents of the most complex materials, i.e., 50DSS. Fig. 4 shows a SEM micrograph of this water-cooled material. The coarse ferrite grains and the areas corresponding to the mixed constituent appeared hardly etching. EDS analysis confirmed this picture (Table 2). High concentration of chromium in the ferrite and nickel in large proportions in the austenite were observed. Molybdenum showed higher concentration in austenite though they stabilize the ferrite. It can be outlined an explanation to this phenomenon which is based on the composition of the base powders. Molybdenum is only present in austenitic powders and only by diffusion, some atoms move to the ferritic powders. The mixed constituent composition was intermediate among them and according to the Schaffler's diagram the present phases were austenite, ferrite and martensite. Similar microstructure has been obtained for vacuum sintered duplex SS 50/50 obtained from premixed of $\text{X}_2\text{Cr NiMo 17-2-2}$ and X_6Cr_{17} [23].

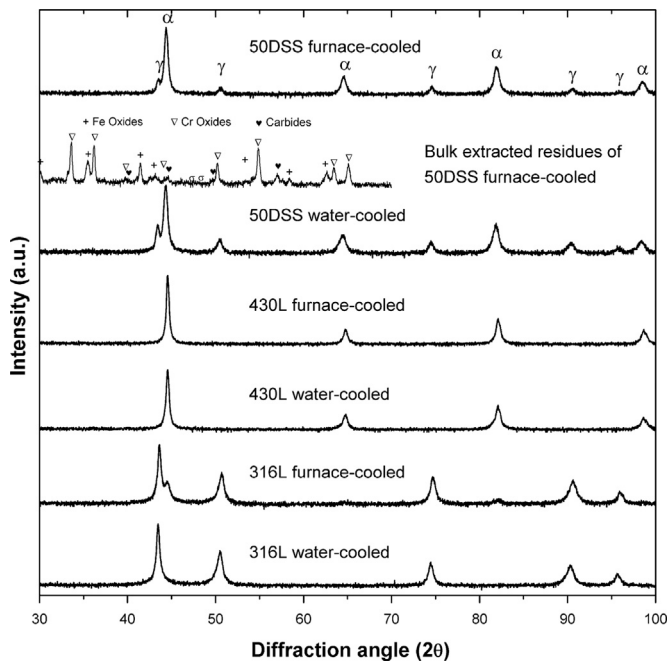


Fig. 3. X-ray diffractograms of furnace- and water-cooled samples and bulk extracted residues of furnace-cooled 50DSS.

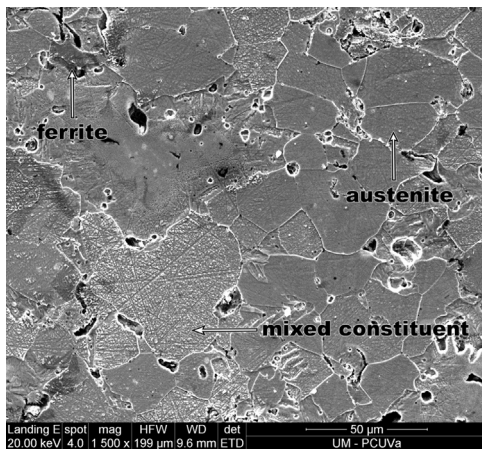


Fig. 4. SEM micrograph of water-cooled 50DSS.

Table 2
EDS results for water-cooled 50DSS. Chemical composition in wt%.

Chemical elements	Ferrite	Mixed constituent	Austenite	Precipitates
Si	0.48	0.40	0.53	10.24
Mo	0.62	0.81	1.09	0.6
Cr	16.64	15.80	14.34	14.56
Fe	79.30	77.45	71.25	65.22
Ni	2.87	5.54	12.79	3.68
O	–	–	–	5.71

3.2. Tensile and hardness tests

Tensile curves were obtained for every sample. For furnace-cooled samples, the influence of compaction pressure was more remarkable for the austenitic and ferritic grades. An increase of tensile strength and ductility was observed when the compaction pressure increased, Fig. 5. This tendency is more evident for the furnace-cooled ferritic and austenitic grades. For duplex SS an improvement of mechanical properties as compared to base materials was observed. For water-cooled samples, an important

mechanical improvement was registered for all compositions and the effect of compaction pressure was less significant.

An improvement of mechanical properties for duplex SS, as compared with the base materials, was observed. However, for water-cooled samples, duplex SS showed the best strength resistance but the ductility was lower than for austenitic and ferritic grades. In this case, the higher amount of martensite phase observed inside of mixed constituent could explain this behavior. The 316L and 430L samples kept its more ductile behavior while a mechanical reinforcement was registered for water-cooled samples.

Finally, the cooling rate was the more important factor on mechanical properties for austenitic and ferritic materials. A strong increase of strength resistance and ductility appeared for water-cooled samples. For duplex SS the cooling rate was less important although water-cooled samples showed the best mechanical behavior in all conditions. Therefore, the use of high compaction pressure and water-cooling promoted the best mechanical results for all compositions.

Hardness measurements indicate that the compaction pressure was an important variable, Fig. 6. As expected because of the porosity all the grades compacted at 750 MPa gave higher hardness than those compacted at 650 MPa. Furthermore, water-cooling process clearly induced an increase in hardness. Duplex SS showed higher hardness than base materials for all conditions. It is deduced that there is a direct correlation between tensile test results and hardness measurements.

4. Discussion

As it is expected the compaction pressure is the variable affecting the porosity while sinter-cooling it is found that barely affects. It is a reasonable result since porosity reduction is a slow process based on diffusion, which even gets less relevant as temperature decreases. Water-cooling is a very fast step but also furnace-cooling are done in a relatively short period of time.

The mechanical properties of any material strongly depend on its microstructural features, which are determined by two factors: chemical composition and sinter-cooling rate.

It has been observed that the degree of precipitation is low for every sample but also that this tendency is lower for water-cooling process since the time for precipitation is reduced.

For furnace-cooled 430L, single grains of ferrite are observed while for furnace-cooled 316L, austenite in large amount is present but the X-ray diffractogram also indicates small contents of ferrite and some precipitation. This might be due to the typical transformation of austenite in α phase plus carbides. For furnace-cooled 50DSS, also a mixed constituent is identified. This is expected in the sense that the duplex is formed by a mixture of austenitic and ferritic powders. Therefore, for these powders of different chemical composition in direct contact, an interdiffusion mechanism is taking place. The EDS analysis confirms the diffusion of Ni and Mo from the austenitic powder and the diffusion of Cr from the ferritic powder. Consequently, there are zones close to the contact area of the particles where the chemical composition is not that of ferrite or austenite but, following the Schaffler's diagram, they are zones with a mixture of very small grains of austenite, ferrite and, in some situations, martensite that is generally called mixed constituent [25].

Water-cooling is a fast process. Therefore, the typical precipitation and decomposition of the austenite cannot take place. This is why, for the 430L and 316L, the respective microstructure shows almost entirely grains of one type, either ferrite or austenite. For water-cooled 50DSS, again the microstructure has its origin in the mixing of the microstructures of the base materials

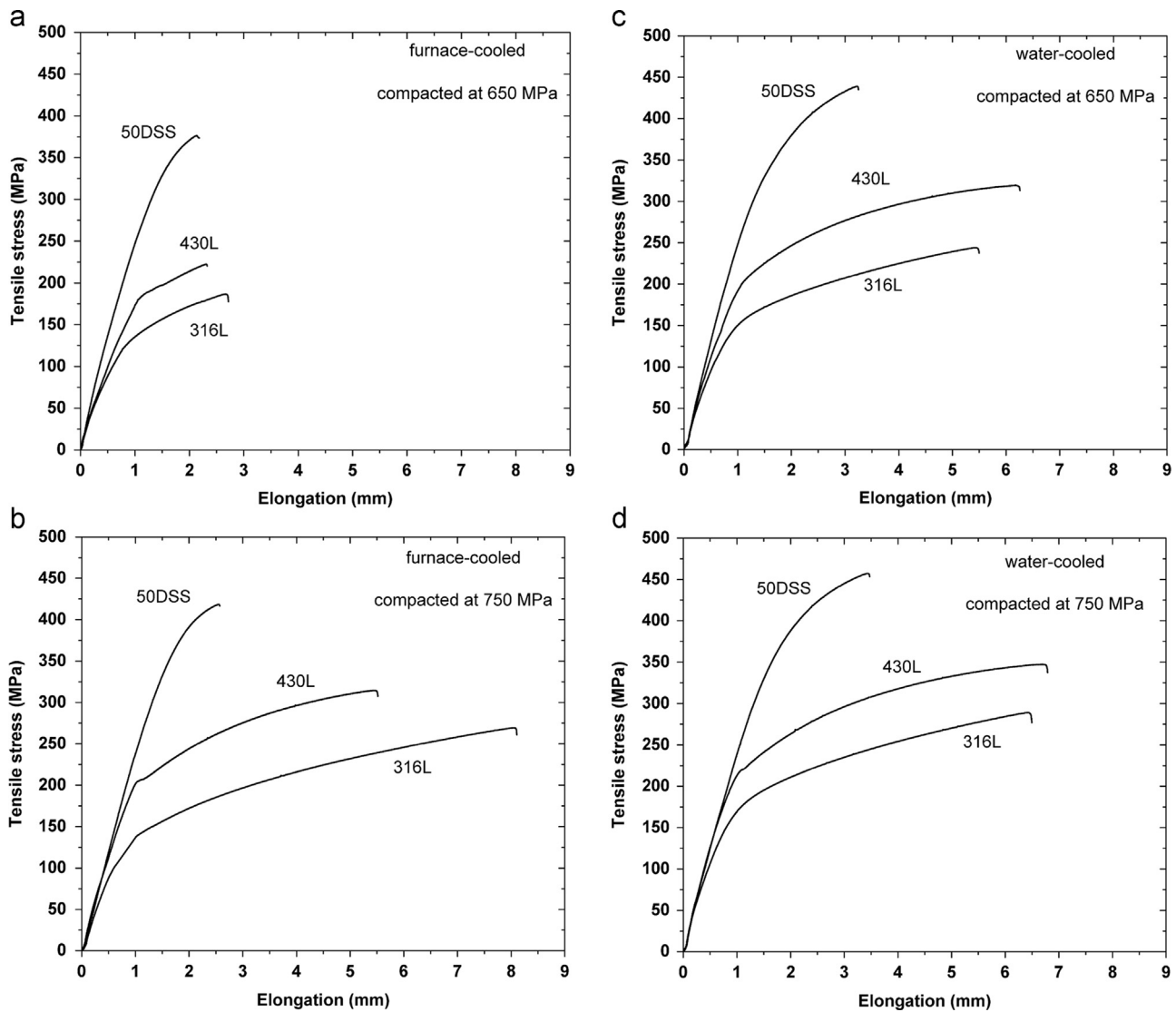


Fig. 5. Tensile curves of furnace-cooled samples (a) compacted at 650 MPa, (b) compacted at 750 MPa and water-cooled samples, (c) compacted at 650 MPa and (d) compacted at 750 MPa.

but with some peculiarities. In this case, the content of austenite and mixed constituent increase while correspondingly the content of ferrite decreases. The different microstructures discussed here must necessarily promote different mechanical behavior for each material.

Regarding the processing parameters, it is deduced that compacting at 750 MPa the materials show higher tensile strength and ductility. As expected, porosity is playing a relevant role: the lower the porosity, the higher the tensile strength. This result is common for the two base materials. Nevertheless, this effect is not so relevant for the duplex SS since the decrease in porosity when the compaction pressure increases is also not so significant than for austenitic and ferritic types. Moreover, the duplex stainless steels show higher tensile strength than the base materials for all sintering conditions. The solid solution hardening of Ni and Mo of the ferrite phase, the internal strain hardening between ferrite and austenite due to different coefficient of thermal expansion and the interdiffusion at particles boundary that originated the mixed constituent can explain the increase of mechanical properties as compared with the monophasic austenitic or ferritic SS.

The sinter-cooling rate is an important factor on the mechanical properties, especially for the two base materials. The tensile strength of water-cooled samples is higher than for those furnace-

cooled. For water-cooled 430L and 316L, the improvement on mechanical properties can be based on the low amount of chromium carbide precipitates and the fine grain. The water-cooled duplex SS shows higher strength resistance but lower ductility than base materials that can be due to the higher amount of martensite phase, which is inside of the mixed constituent.

Therefore, although it is generally accepted that the porosity is the most important factor to define the mechanical properties of PM steels, it can be concluded that their mechanical properties depend as much on the composition and sinter-cooling conditions (i.e., microstructure) as on the degree of porosity.

Focusing the study on the hardness of the materials, for furnace-cooled base materials, the compaction pressure at 750 MPa gives an improvement on hardness. The reduction in porosity is the key to explain this result since the microstructure for each materials does not change. The compaction pressure is obviously a relevant parameter for the decrease in porosity of the PM material. It is clear that decreasing porosity improves all the mechanical properties, including hardness.

It can be observed that duplex SS exhibits the maximum hardness since these samples showed mixed constituent with martensite phase in it. On the contrary, 316L is the sample with the lowest hardness due to its high content in austenite with lower

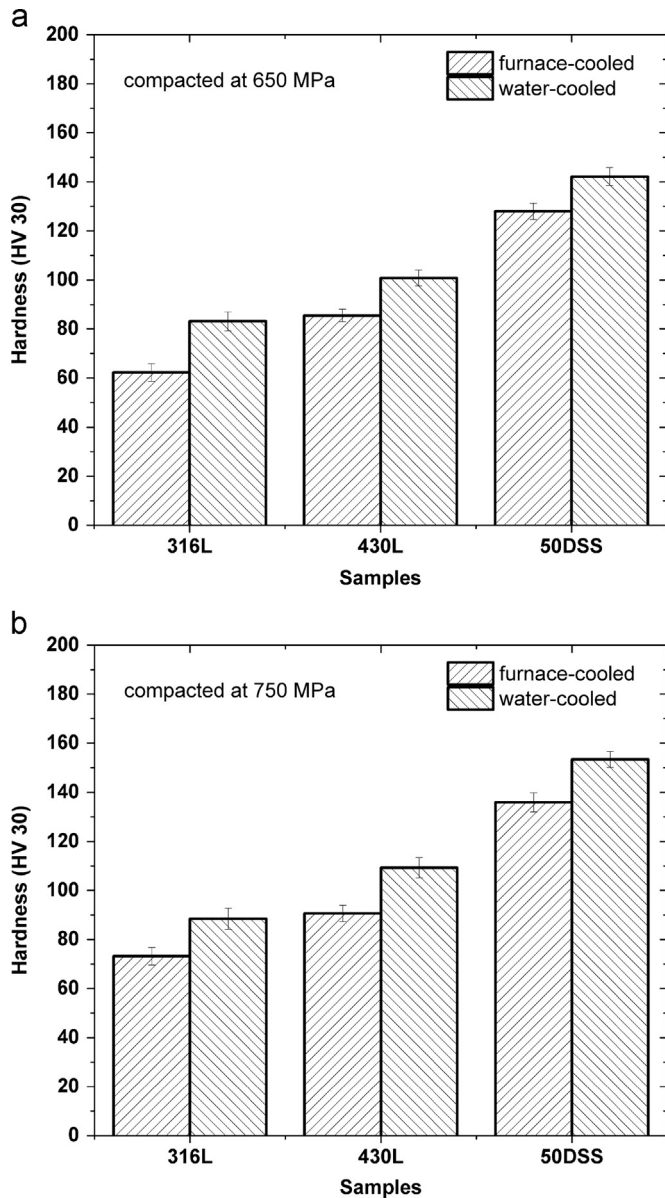


Fig. 6. Vickers hardness of the samples compacted at (a) 650 MPa and (b) 750 MPa.

hardness than ferrite phase.

The second point to analyse is the effect of the sinter-cooling rate. In every case, the hardness increases with the cooling rate. Water-cooling induces a decrease of porosity and grain size for austenitic and ferritic samples, which could explain the increase of hardness. For duplex SS the higher amount of mixed constituent for samples with rapid cooling explain the observed hardening.

5. Conclusions

Two simple stainless steels, austenitic and ferritic, and one duplex SS have been studied. In order to obtain different microstructures for every sample, two sinter-cooling rates were set. Porosity barely changed for the two sinter-cooling processes. However, as expected, it did by increasing the compaction pressure. The furnace-cooled microstructures of the base materials (316L and 430L) showed respectively the typical austenite and ferrite phases plus some precipitates. On the contrary, water-

cooling promoted a cleaner austenite phase for 316L but for 430L the amount of precipitates was higher. Therefore, water-cooling is recommended for the austenitic SS but not for 430L if a clean monophasic microstructure is searched.

The duplex SS showed a more complex microstructure for the two sinter-cooling processes. Austenite, ferrite plus some precipitates were always present but also the so-called mixed constituent was identified. This mixed constituent was mainly composed of austenite and ferrite for the furnace-cooled sample but for the water-cooled, it was additionally observed martensite. Finally, the amount of ferrite grains was higher for the furnace-cooled sample than for the water-cooled one.

Tensile test were done for every sample. The influence of compaction pressure was more remarkable for the austenitic and ferritic types. An increase of tensile strength and ductility was observed when the compaction pressure increased. The reduction in porosity was the cause of this expected behavior. Water-cooling promoted higher tensile strengths, therefore this is the recommended process. These mechanical properties have been related with the microstructure of the materials. It has also been found that hardness correlates with tensile properties.

References

- [1] R.M. German, *Powder Metallurgy of Iron and Steel*, John Wiley, NY (1998), p. 437–460.
- [2] M. Aksoy, V. Kuzucu, M.H. Korfut, *Wear* 211 (1997) 265–270.
- [3] A. Bautista, F. Velasco, S. Guzman, D. de la Fuente, F. Cayuela, M. Morcillo, *Rev. Metal.* 42 (2006) 175–184.
- [4] P. Samal, I. Hauer, O. Mars, B. Maroli, *Met. Powder Rep.* 61 (2006) 22–29.
- [5] P. Datta, G.S. Upadhyaya, *Mater. Chem. Phys.* 67 (2001) 234–242.
- [6] C. García, F. Martín, Y. Blanco, M.P. de Tiedra, M.L. Aparicio, *Corros. Sci.* 51 (2009) 76–86.
- [7] R. Dakhlaoui, A. Baczmanski, C. Braham, S. Wroński, K. Wierzbanski, E. C. Oliver, *Acta Mater.* 54 (2006) 5027–5039.
- [8] L. Woei-Shian, L. Chi-Feng, L. Tsung-Ju, *Mater. Charact.* 58 (2007) 363–370.
- [9] R. Mariappan, S. Kumaran, T. Srinivasa Rao, *Mater. Sci. Eng. A* 517 (2009) 328–333.
- [10] N. Kurgan, R. Varol, *Powder Technol.* 201 (2010) 242–247.
- [11] S. Pandya, K.S. Ramakrishana, A. Raja Annamalai, A. Upadhyaya, *Mater. Sci. Eng. A* 556 (2012) 271–277.
- [12] W.F. Wang, M.J. Wu, *Mater. Sci. Eng. A* 425 (2006) 167–171.
- [13] M. Campos, A. Bautista, D. Cáceres, J. Abenojar, J.M. Torralba, *J. Eur. Ceram. Soc.* 23 (2003) 2813–2819.
- [14] D. Uzunsoy, *Mater. Lett.* 61 (2007) 10–15.
- [15] P. Datta, G.S. Upadhyaya, *Met. Powder Rep.* 29 (1999) 26–29.
- [16] J. Kazior, M. Nykiel, T. Pieczonka, T. Marcu Puscas, A. Molinari, J. Mater. Process. Technol. 157–158 (2004) 712–717.
- [17] C. García, F. Martín, P. de Tiedra, L. García Cambronero, *Corros. Sci.* 49 (2007) 1718–1736.
- [18] F. Martín, C. García, P. de Tiedra, Y. Blanco, M.L. Aparicio, *Corrosion* 64 (2008) 70–82.
- [19] T. Marcu Puscas, A. Molinari, J. Kazior, T. Pieczonka, M. Nykiel, *Powder Metall.* 44 (2001) 48–52.
- [20] D. Ornato, *Powder Metall.* 45 (2002) 290–293.
- [21] C.J. Múñez, M.V. Utrilla, A. Ureña, *J. Alloy. Compd.* 463 (2008) 552–558.
- [22] M.R. Raza, F. Ahmad, M.A. Omar, R.M. German, *J. Mater. Process. Technol.* 212 (2012) 164–170.
- [23] L.A. Dobrzanski, Z. Brytan, M.A. Grande, M. Rosso, E.J. Pallavicini, *J. Mater. Process. Technol.* 162–163 (2005) 286–292.
- [24] L.A. Dobrzanski, Z. Brytan, M.A. Grande, M. Rosso, *J. Mater. Process. Technol.* 191 (2007) 161–164.
- [25] C. García, F. Martín, Y. Blanco, M.P. de Tiedra, M.L. Aparicio, *Metall. Mater. Trans. A* 40 (2009) 292–301.
- [26] C. García, F. Martín, Y. Blanco, M.L. Aparicio, *Corros. Sci.* 52 (2010) 3725–3737.
- [27] C. García, F. Martín, Y. Blanco, *Corros. Sci.* 61 (2012) 45–52.
- [28] F. Martín, C. García, Y. Blanco, *Mater. Sci. Eng. A* 528 (2011) 8500–8511.
- [29] ISO 2740:2007, *Sintered Metal Materials, Excluding Hardmetals – Tensile Test Pieces*.
- [30] ASTM Standard A262-91, *Standard Practice for Detecting Susceptibility to Intergranular Attack on Austenitic Stainless Steels*, ASTM, Philadelphia (1993), p. 1–18.
- [31] ISO 6892-1:2009, *Metallic Materials – Tensile Testing – Part 1: Method of Test at Room Temperature*.